Early–Middle Eocene exhumation of the Trans-Himalayan Ladakh Batholith, and the India–Asia convergence

Rajeev Kumar[1], A. K. Jain[2,*], Nand Lal[3] and Sandeep Singh[1]

[1]Department of Earth Sciences, Indian Institute of Technology Roorkee, Roorkee 247 667, India
[2]CSIR-Central Building Research Institute, Roorkee 247 667, India
[3]Sri Sri University, Cuttack 754 006, India

Very fast Early–Middle Eocene exhumation of the Trans-Himalayan Ladakh Batholith (LB) is revealed by new Rb–Sr biotite and zircon fission-track ages along with the already published ages on these minerals. Exhumation peaked at 3.5 ± 0.9 mm/a between 50–45 Ma (^{40}Ar/^{39}Ar hornblende ages) and 48–45 Ma (Rb–Sr biotite ages) as a consequence of the India–Asia convergence. It was followed by deceleration at a rate of 1.2 ± 0.2 mm/a until 43–42 Ma (zircon FT ages), like the Deosai batholith in the west. Exhumation rates finally decreased during Oligocene to a minimum of ~0.1 mm/a before a mild late Miocene–Holocene acceleration. Lower-Middle Eocene exhumation of the LB was tectonically controlled by slab break-off of the Neo-Tethys oceanic lithosphere and underthrusting of the Himalayan Metamorphic Belt.

Keywords: Early–Middle Eocene exhumation, fission track, Ladakh Batholith, tectonics.

EXHUMATION of deeply-buried rock sequences is one of the challenging geodynamic problems in convergent orogens, where both tectonics and erosion can cause these, either independently or in combination. Tectonic-dependent exhumation models range from low-angle ductile extensional faults, syn-convergent normal faulting or crustal overthickening with low-angle ductile flow[1–3]. However, erosion gained recent importance as an effective alternative mechanism in climatic-wet active convergence zones, where fluvial drainage system removes the eroded detritus[4,5].

In the Himalayan domain, tectonically driven exhumation is caused by ductile thrusting along the Main Central Thrust (MCT)[6,7], fold amplification[7], out-of-sequence thrusting, Himalayan discontinuities[8], and crustal overthrusting along the Main Himalayan Thrust (MHT) and its ramp-flat geometry[9], while its northern boundary underwent exhumation by extensional faulting[10,11]. Alternatively, architecture of the Himalaya has resulted from a combination of tectonics, focused precipitation, climate-driven erosion and/or recent glacially enhanced denudation[5,9,12].

In contrast to the Himalayan domain, exhumation models are inadequate for the Trans-Himalayan Andean-type Ladakh Batholith (LB), which was emplaced during Early Cretaceous–Lower Eocene (Figure 1)[13–17], and subsequently cooled and exhumed either during Early–Middle Eocene[18–20] or Early Miocene[21,22]. These models range from effects of thrusting along the MCT[21], its northwards tilting[22] or effects of the Karakoram Fault Zone[18]. ^{40}Ar/^{39}Ar hornblende, biotite and K-feldspar ages between 52 and 44 Ma record an Early Eocene rapid cooling and a slow cooling between c. 30 and 10 Ma (refs 15, 18), like the Deosai plateau in the west[20]. In contrast, (U–Th)/He zircon–apatite and apatite fission-track (AFT) ages reveal rapid Early Miocene 22 ± 2 Ma cooling of the LB[21,22].

Radioactive decay of a parent nuclide and the accumulation of a corresponding daughter product are used to date either the crystallization age or cooling age of a mineral in the disciplines of geochronology and thermochronology[23]. The latter uses many thermochronometers whose closure temperatures range from ~900°C (U–Pb zircon) to as low as ~50°C (U–Th/He apatite) (see ref. 23 for review). In this article, we present new Rb–Sr biotite and zircon fission-track (ZFT) mineral ages along with length measurements of apatite fission-track (AFT) from the LB. These data are integrated with already published mineral ages (Supplementary Table 1) for deciphering cooling and exhumation histories of the LB.

Geological framework

The Trans-Himalayan Mountains expose a long linear LB belt in Kargil–Leh–Demchuk region in India and the Kohistan–Deosai Batholith of Astor–Deosai–Skardu region in Pakistan[24,25]. This belt extends eastwards as the Kailash Tonalite and the Gangdese pluton in southern Tibet[26,27], and the Lohit Batholith in Mishmi Hills, Arunachal Himalaya[25] (Figure 1 *a*). LB is bound by the Indus Tsangpo Suture Zone (ITSZ) along its southern margin,

*For correspondence. (e-mail: himalfes@gmail.com)

while the Shyok Suture Zone (SSZ) frames its northern margin. These sutures demarcate Early Cretaceous subduction of the Neo-Tethyan oceanic lithosphere[28] and closure of this ocean between the Indian and Asian Plates[24,29–35] (Figure 1 *a* and *b*). The batholith trends WNW–ESE for nearly 600 km in a 30–80 km wide belt (Figure 1 *b*), with an exposed thickness of ~2 km. It is mainly of diorite–granodiorite and granite composition with I-type geochemistry, and crystallized between ~100 and 47 Ma with a dominant phase at ~58 Ma (refs 26, 36–38).

A N25°W-trending and ~2 km wide ductile dextral transpressional Thanglasgo Shear Zone (TSZ) (Figure 1 *b*) deforms the batholith and contains mylonite, asymmetric feldspar augen, S-C shear fabric and NW-plunging lineation[15]. However, this shear zone becomes a thrust[22,39] in the southeast around Leh.

SSZ contains dismembered ultramafics–mafic and sedimentary bodies along the Nubra–Shyok Valleys, where these are thrust over LB or Shyok Volcanics[16,40]. Narrow strips of mylonite, volcanics, sediments and serpentinite characterize the dextral transpressional Karakoram Shear Zone (KSZ) between SSZ and Karakoram batholith–metamorphics complex along the southern Asian Plate margin with initial thrust movements (Figure 1 *b*)[34].

In the south, ITSZ contains tectonically imbricated ophiolite, Triassic to Upper Cretaceous Lamayuru Formation, Jurassic–Lower Cretaceous (164–95 Ma) volcano-sedimentary Nindam Formation, deposited on an intra-oceanic

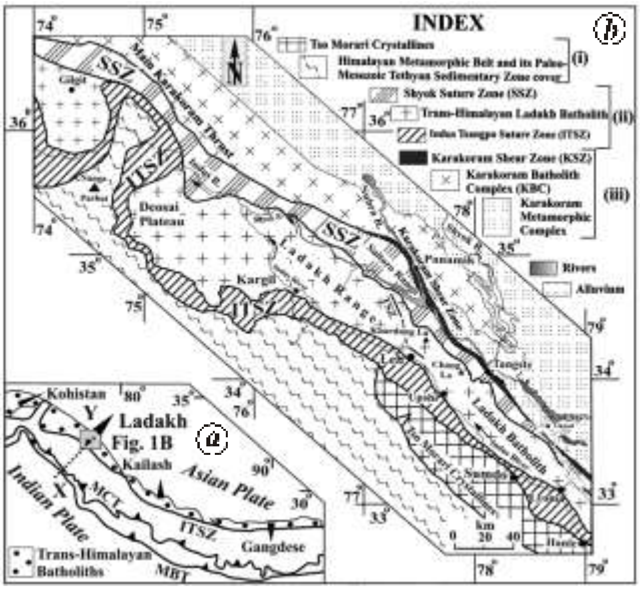

Figure 1. ***a***, Tectonics of the Trans–Himalayan Kohistan, Ladakh, Kailash and Gangdese batholiths along southern margin of the Asian Plate, bounded by the Indus Tsangpo Suture Zone (ITSZ) and Shyok Suture Zone (SSZ). Box shows the study area. ***b***, Geological map of the Ladakh Batholith[34,39] with Thanglasgo Shear Zone (TSZ)[15]. UHP metamorphosed Indian Plate is exposed in Tso Morari towards southwest.

Dras–Shyok volcanic island arc, the Nidar ophiolitic complex (139.6 ± 32.2 Ma), and unconformably overlying Indus Group Eocene sedimentary sequence[19,25,41,42]. Further south of ITSZ, the Himalayan Metamorphic Belt (HMB) underwent UHP metamorphism in Tso Morari at 53.3 ± 0.7 Ma (refs 43, 44), and southward ductile shearing with older pre-Main Central Thrust (MCT) discontinuities[8]. MCT resulted in thrusting HMB over the Proterozoic Lesser Himalayan belt, which overrides the Cenozoic Sub-Himalayan belt, and the latter on to the Indo-Gangetic Plains[14,32,39].

Thermochronology, methods and modelling

Extensive sampling of LB was carried out along three Leh–Khardung La, Kharu–Chang La and Lyoma–Hanle traverses (Supplementary Figure 1). The first two are vertical profiles across the batholith, which are more suitable for deciphering the cooling and exhumation histories. Our earlier effort on fission-track (FT) dating of LB was confined to 3 zircon and 30 apatite age determinations[45]. These samples are further processed for 8 Rb–Sr biotite ages, 15 ZFT ages, and FT-length measurements on 7 apatite mounts, following the procedures given in Supplementary SM2(a–d). Detailed methodologies for estimating closure temperatures, calculation of exhumation rates, determination of geothermal gradients and thermal modelilng are elaborated in Supplementary SM3(a–f).

Results

Eight Rb–Sr biotite samples from different elevations of LB yield ages from 48.0 ± 1 to 45.0 ± 0.1 Ma in a narrow range with an overall weighted mean (OWM = 46.2 ± 0.5–1σ; Table 1; Figure 2). Two biotite ages from the Leh–Khardung La section are of 46.0 ± 0.1 Ma, while the remaining 6 samples lie between 48.0 ± 1.0 and 45.0 ± 0.1 Ma from Kharu–Chang La traverse.

Fifteen new ZFT ages from different elevations of the batholith range between 48.1 ± 2.9 and 37.2 ± 2.2 Ma (1σ; OWM = 43.0 ± 0.5 Ma, Table 2; Figure 2). Out of these, 8 samples from the Leh–Khardung La section yield ages between 48.1 ± 2.9 and 40.4 ± 1.5 Ma, while the remaining 7 samples from the Kharu–Chang La range between 45.2 ± 1.5 and 37.2 ± 2.2 Ma. New results are consistent with our 3 previously published zircon ages. Most of these ages fall between 45.2 ± 1.5 and 40.3 ± 2.3 Ma with an OWM = 43.0 ± 0.5 Ma. These ages remain unaffected by any tectonic boundaries (Figure 3 *a*). About 150 km west of Leh–Khardung section, the Kargil pluton gave ZFT ages of 45.2 ± 3.1 and 41.4 ± 2.2 Ma (ref. 46) (Supplementary Table 1). These ages represent an overall single uniform population of the batholith, unlike the one isolated 26.2 ± 1.8 Ma age near Khardung La[21] (Figure 3 *a*).

Table 1. Rb–Sr ages of biotite from the Ladakh Batholith, Ladakh

Sample no.	Mineral/WR*	Rb (ppm)	Sr (ppm)	$^{87}Rb/^{86}Sr$	$^{87}Sr/^{86}Sr$	Age (Ma) (1σ)
Leh-Khardung La section						
NS3/5	WR	19.03	143.40	0.3839	0.704583	46.1 ± 0.1
	Biotite	269.7	52.8	13.9896	0.713492	
NS5/12	WR	44.28	56.32	2.2744	0.705213	46.0 ± 0.1
	Biotite	347.9	29.4	34.2299	0.726107	
Kharu-Chang La section						
LB8/23	WR	42.39	358.40	0.3427	0.704478	47.9 ± 0.1
	Biotite	271.6	54.1	14.7967	0.714309	
LB9/27	WR	1.22	108.50	0.2346	0.70777	48.0 ± 1.0
	Biotite	493.1	29.9	48.5107	0.740672	
LB10/28	WR	66.76	106.94	1.8054	0.706401	45.2 ± 0.9
	Biotite	633.3	6.6	280.33	0.885223	
LB11/29	WR	42.79	171.81	0.7197	0.705169	45.0 ± 0.1
	Biotite	241.8	46.2	15.1200	0.714373	
LB14/32	WR	59.49	179.49	0.9658	0.705017	46.0 ± 0.1
	Biotite	311.5	40.7	22.0952	0.718834	
LB15/33	WR	72.37	114.98	1.8189	0.705769	47.2 ± 1
	Biotite	514.7	29.8	53.0815	0.740125	
Overall weighted mean (OWM) of biotite ages						46.2 ± 0.5

*Whole-rock.

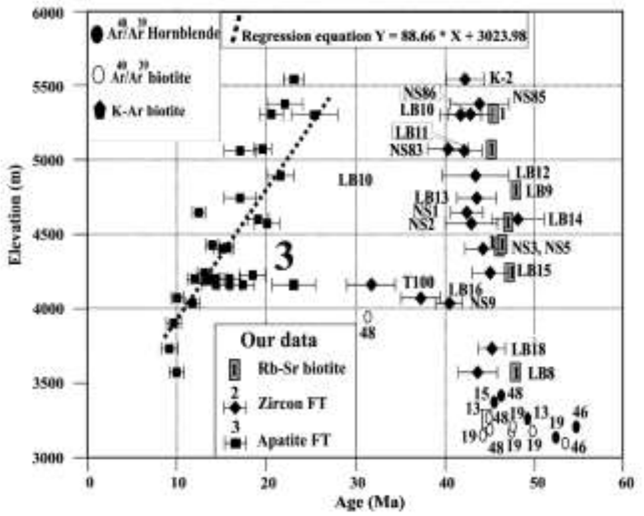

Figure 2. Hornblende, biotite, zircon and apatite ages from the Ladakh Batholith against elevation. Hornblende ages[15,19,46(a),48] (a-K–Ar age, all others $^{40}Ar/^{39}Ar$ ages). Biotite ages[13(b),19,46] (b-K–Ar age, all others $^{40}Ar/^{39}Ar$ ages), 13(c)(Rb–Sr age). Our data: 1–Rb–Sr biotite ages, 2-zircon FT ages also[45], 3-apatite FT ages[45].

Mean FT-length measurements of seven apatite samples vary from 12.6 ± 0.2 to 10.5 ± 0.2 μm (SD = 1.7 to 1.3 μm) with consistent unimodal length distribution (Table 3).

Discussion

Cooling history of LB

After pulsative crystallization of the LB between ~100 and 41 Ma (refs 15, 17, 24, 26, 36, 37, 47) with main phase at ~58.0 Ma (ref. 38) (U–Pb zircon ages), the batholith initially cooled by normal conductive cooling and then underwent much faster cooling, resulting from tectonically controlled uplift due to convergence of the India–Asia Plates.

Our published 30 AFT ages of LB from these sections varied between 25.4 ± 2.6 and 9.2 ± 0.9 Ma (1σ), with oldest ages of 25.4 ± 2.6 and 23.1 ± 1.1 Ma obtained from highest Khardung La and Chang La, and the youngest ages of 11.8 ± 1.1 and 9.2 ± 0.9 Ma from near the Indus River[45] (Figure 3 *b*). The easternmost Lyoma section with no elevation difference has AFT ages between 18.5 ± 1.4 and 12.1 ± 1.0 Ma (Supplementary Table 1).

Eight new Rb–Sr biotite ages (47.98 ± 0.97 to 45.0 ± 0.13 Ma–OWM 46.2 ± 0.50 Ma) from LB are indistinguishable from already-published $^{40}Ar/^{39}Ar$ hornblende ages between 52.2 ± 0.3 and 44.3 ± 0.1 Ma (refs 15, 19, 48) and biotite ages between 49.2 ± 0.08 and 32.6 ± 0.2 Ma (refs 19, 24, 49) (Supplementary Table 1), which were determined by Rb–Sr and $^{40}Ar/^{39}Ar$ (including K–Ar) methods (Figure 2). It is, therefore, evident that batholith cooled almost instantly between $^{40}Ar/^{39}Ar$ hornblende (500 ± 50°C) and Rb–Sr biotite (340 ± 30°C) closure temperatures from 52–44 Ma to ~46.0 Ma at a very fast rate of ~105°C/Ma in contrast to slower cooling within the Himalayan orogen[9,12].

New zircon FT ages (OWM = 43.0 ± 0.5 Ma, Table 2) constrain its low-temperature cooling history (Figure 3 *a*). When ZFT ages from the Kargil pluton are taken into consideration[46] (Supplementary Table 1), the batholiths yields an overall single uniform ZFT age population.

Table 2. Zircon fission-track (ZFT) data of from the Ladakh Batholith, Ladakh

Sample code	Lab code	Elevation (m)	No. of crystals	Track densities: Spontaneous ρ_s (N_s)	Track densities: Induced ρ_i (N_i)	$P(\chi^2)$ % age	Glass dosimeter ρ_d (N_d)	Age (Ma) ($\pm 1\sigma$)
Leh–Khardung La section								
NS 1/1	NS 1	4645	27	3.529 (1025)	8.329 (2430)	61.66	0.6795 (2718)	42.4 ± 1.8
NS 2/3	NS 2	4600	11	4.367 (402)	12.47 (1147)	84.33	0.9276 (4638)	48.1 ± 2.9
NS 5/12	NS 5	4401	16	2.871 (693)	8.949 (2154)	54.72	0.9276 (4638)	44.2 ± 2.0
NS 9/20	NS 9	4038	43	2.945 (1248)	8.880 (3808)	100.00	0.8323 (3329)	40.4 ± 1.5
NS83/157	NS 83	5071	15	3.760 (496)	9.180 (1238)	80.62	0.6795 (2718)	40.3 ± 2.3
NS85/162	NS 85	5375	05	4.353 (234)	12.980 (734)	58.30	0.9276 (4638)	43.8 ± 3.3
NS86/163	NS 86	5305	11	4.135 (408)	13.210 (1310)	94.84	0.9276 (4638)	42.8 ± 2.5
K-2	K-2	5540	16	4.027 (677)	9.584 (1614)	18.30	0.6795 (2718)	42.2 ± 2.1
Kharu–Chang La section								
LB 8/23	8/23	3572	14	3.023 (613)	8.597 (1730)	50.85	0.8323 (3329)	43.6 ± 2.2
LB10/28*	Zr 14	5301	09	9.5614 (545)	22.491 (1282)	50.00	0.6632 (2653)	41.7 ± 2.3
LB11/29	11	5060	12	3.809 (630)	12.820 (2055)	11.38	0.9276 (4638)	42.1 ± 2.0
LB12/30*	12/30z	4893	04	9.2609 (213)	20.9565 (482)	50.00	0.6632 (2653)	43.4 ± 3.7
LB13/31	13/31	4742	15	3.517 (578)	9.935 (1635)	42.77	0.8323 (3329)	43.5 ± 2.2
LB14/32	14	4409	05	4.506 (300)	14.750 (961)	36.57	0.9276 (4638)	42.9 ± 2.9
LB15/33	15	4241	13	0.5120 (722)	15.350 (2201)	32.59	0.9276 (4638)	45.0 ± 2.0
LB16/34	16/34	4072	15	4.026 (409)	13.770 (1353)	98.11	0.8323 (3329)	37.2 ± 2.2
LB18/36	18/36	3732	29	3.433 (1627)	10.440 (4923)	76.00	0.9276 (4638)	45.2 ± 1.5
Lyoma–Hanle section								
T100/350*	Zr15	4160	02	4.875 (195)	15.10 (604)	50.0	0.6632 (2653)	31.7 ± 2.7

OWM: 42.7 ± 0.5 Ma
OWM (excluding sample no. 18) 43.0 ± 0.5 Ma

*Data from Kumar *et al.*[45]. ρ_s, spontaneous fission track density and are 10^6 tr/cm^{-2}. N_s, number of spontaneous tracks counted. N_i, number of induced tracks counted. ρ_i, induced track density in mica detector. ρ_d, induced track density in glass dosimeter. $P(\chi^2)$, probability of obtaining the observed χ^2 value for (number of crystals-1) degrees of freedom, which is quoted nearest to 5%. The ages were calculated using $T = 1/\lambda_d \ln[1 + G\zeta\lambda d(\rho_s\rho_d)/\rho_i]$, where λ_d = Total decay constant of U^{238} (= 1.55125 × 10^{-10} per year), G, geometry factor (= 0.5, as the spontaneous tracks were counted under 4π conditions), ρ_s, spontaneous track density, ζ, zeta calibration factor (zeta value used = 296.96 ± 8.18), measured by Kumar[45] on standard glass corning 5 (CN5) prepared by Dr J. W. H. Schreurs at Corning Glass Works, Corning, New York, USA.

Table 3. Apatite mean fission track-length data, Ladakh Batholith

Sample code	Elevation (m)	AFT age (Ma)*	Mean track length (μm)	Standard deviation (μm)	No. of tracks measured
NS9/20	4038	11.8 ± 0.8	11.42 ± 0.19	1.41	53
K-2	5440	23.1 ± 1.1	12.60 ± 0.19	1.72	61
LB 10/28	5301	25.4 ± 2.6	12.50 ± 0.24	1.72	50
LB14/32	4409	15.6 ± 0.8	11.57 ± 1.8	1.78	32
LB18/36	3732	9.2 ± 0.9	11.00 ± 1.7	1.72	39
T93/334	4200	13.7 ± 1.0	10.5 ± 0.23	1.38	35
T100/350	4160	17.4 ± 1.3	11.3 ± 0.23	1.31	31

Thus, LB cooled from Rb–Sr biotite closure temperature (340 ± 30°C at ~46.0 Ma) to the ZFT closure temperature (230 ± 20°C at ~43.0 Ma) at 34 ± 13°C/Ma (Supplementary SM3(d)).

For deciphering the low temperature cooling history, new ZFT ages are considered with our apatite[45] and published FT data, and zircon and apatite (U–Th)/He (ZHe, AHe) ages[21,22] of the LB and the Deosai Batholith in the west[20]. Thus it covers a temperature range from 230 ± 20 to ~55°C – the annealing temperatures of ZFT and AHe respectively. Our AFT ages from central parts of LB[45] are similar to other AFT ages[21,22] (Figure 3 *b*). The LB crossed ZHe temperature (~200°C) at ~30 Ma (ref. 22) and cooled from 230 ± 20°C at ~43 Ma with a slow rate of ~2°C/Ma in southern and central parts (Figure 4). From central parts of the Deosai Plateau, ZHe ages vary from 39.4 ± 7.4 to 22.1 ± 1.0 Ma from highest to lower elevations. Here, AFT ages range between 27.0 ± 3.5 and 14.6 ± 1.1 Ma and the AHe ages are between 15.1 ± 0.3 and 10.9 ± 1.0 Ma with strong elevation control[20], thus following a systematic decreasing age pattern. From LB, the ZHe ages vary from 30.9 ± 5.8 Ma in the vicinity of

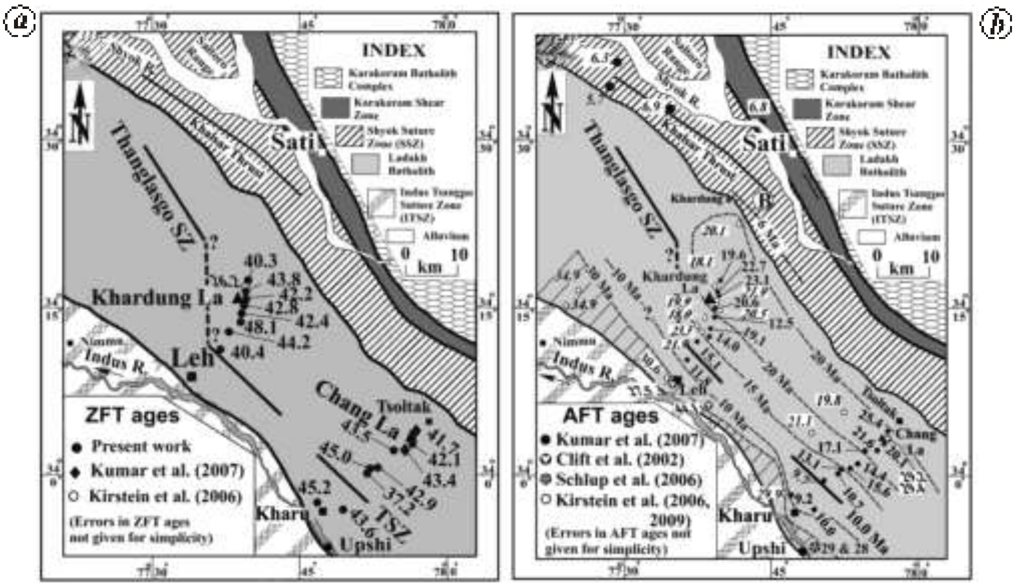

Figure 3. Distribution of fission-track ages across the Ladakh Batholith. ***a***, ZFT ages between Khardung La and Chang La areas around Leh[22,45,this work]. ***b***, AFT ages from Khardung La and Chang La areas around Leh showing distinct isochrones[19,22,45].

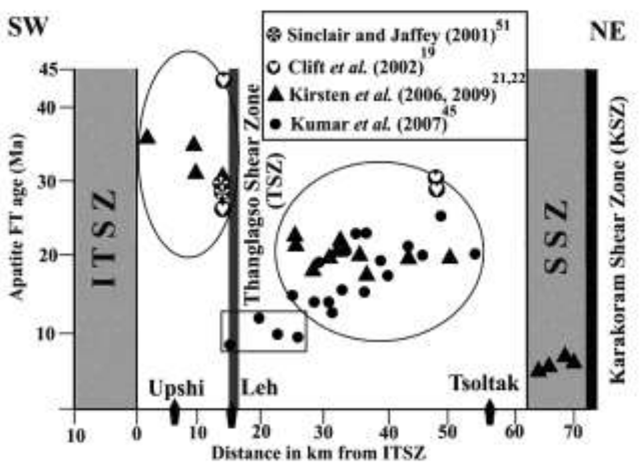

Figure 4. Distance versus age plot of AFT ages from the Ladakh Batholith along Upshi-Tsoltak section paralleling the Kharu-Chang La road. All ages from the Leh–Khardung La section and adjoining regions projected along this section. Note four distinct age groups and role of the TSZ and SSZ in distribution of the AFT ages. Data from various sources, as indicated.

the Indus River to 13.5 ± 1.2 Ma towards KSZ in the north across the batholith, while AHe ages are from 21.8 ± 0.6 to 12 Ma (refs 21, 22). A Late Oligocene cooling happened in the south, while the central part remained hot until Miocene, possibly due to northward tilting of the batholith[22].

^{40}Ar/^{39}Ar K-feldspar ages from an undeformed sample from Chang La are from 49 to 36 Ma between 350 and 150°C (ref. 18) yielded smooth cooling rate of 15°C/Ma. With ZFT–AFT ages of 42 and 25 Ma falling nearly in between, the cooling rate of batholith remained the same till it crossed the ZFT temperature, but it dwindled to 7° ± 2°C when the AFT temperature of 115° ± 20°C was reached.

Though ZFT ages exhibit a consistent pattern, LB underwent perturbations during lowering of its temperature. The AFT age distribution has breaks between 44 and 5 Ma (refs 21, 22, 45) (Supplementary Table 1) and appears to be controlled by the following tectonic features (Figure 4):

(i) Southernmost belt of 9 oldest AFT ages between 44.1 ± 6.3 and 28 ± 3 Ma (refs 21, 22, 50, 51) at the lowermost elevation from 3295 to 4000 m (Supplementary Table 1) between ITSZ and Thanglasgo SZ with very slow cooling and exhumation.

(ii) Group of 4 AFT ages between 11.8 ± 0.8 and 9.2 ± 0.9 Ma (refs 22, 39) within the Thanglasgo SZ with faster cooling. Ductile shearing within this zone records intense deformation with SW-directed thrusting between Leh and Khardung La.

(iii) Nearly uniform AFT ages of 26 samples in central parts between 23.3 ± 2.1 and 18.0 ± 1.4 Ma, indicating its typical AFT age character.

(iv) Youngest northern group of 4 AFT ages between 6.9 ± 5.0 and 5.7 ± 4.8 Ma from granitoids due to late Miocene reactivation of the Karakoram SZ (KSZ).

Inverse modelling, using annealing algorithm and 'HeFTy' program (Supplementary refs 14 and 22), is applied on 7 chemically suitable apatite samples by measuring FT-lengths for calculating the best-possible time-temperature (*t*–*T*) paths of LB. By applying Goodness of Fit (GOF) test (Figure 5), results exhibit an accuracy of >0.9 and a rapid mean cooling rate of ~6–7°C/Ma irrespective of their elevations, till these enter the apatite partial retention zone (APRZ). Here, prolonged residency period is indicated with slow monotonous cooling at a mean rate of ~2–3°C/Ma and another accelerated cooling rate of ~7°C/Ma till these reach the surface. Sample T93/334 did not yield good path with poor statistical GOF test quality. *t–T* paths for high elevation samples (K2–5440 m; LB10/28–5301 m) show that these enter APRZ during 30–28 Ma from their respective ZPRZ, whereas the remaining samples between 4400 and 3700 m show the same cooling steps during 20–18 Ma; these come out of APRZ after prolonged residency at ~2–4 Ma irrespective of elevations and geographical distribution.

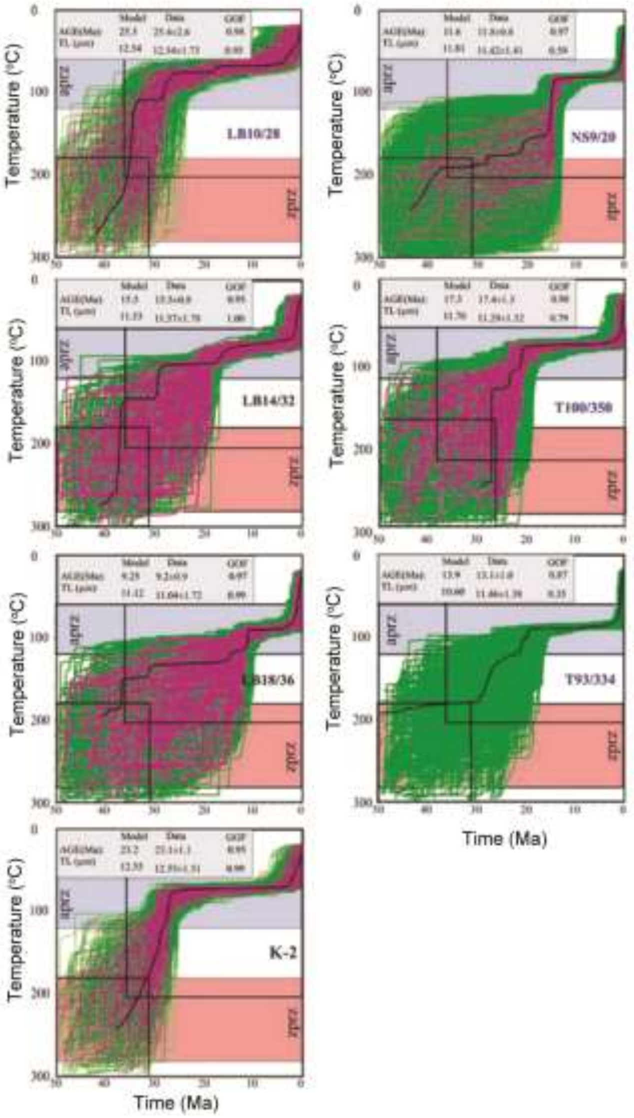

Figure 5. Modelled *t–T* paths for the Ladakh Batholith, using 'HeFTy' program (Supplementary ref. 14) on apatite track-length data. Green: Thermal histories with an acceptable fit. Purple: Thermal histories with a good fit. Black line in centre: best fit to the data. Boxes are *t–T* constraints indicated by zircon FT ages, apatite FT ages and present surface temperatures. Modelled and observed data set along with their correlation, shown as goodness of fit (GOF), are given in top left panel. Purple and pink shaded areas denote APRZ and ZPRZ, respectively.

Exhumation rates

LB crystallized mainly at ~58.0 Ma and attained the $^{40}Ar/^{39}Ar$ hornblende closure temperature at ~50–45 Ma due to magmatic cooling of this body. It witnessed an Early–Middle Eocene very fast exhumation of 3.5 ± 0.9 mm/year between 50–45 and 48–45 Ma – the Rb–Sr biotite age, and decelerated to 1.2 ± 0.4 mm/year to the ZFT age (43.0 ± 0.5 Ma). These are further reduced to nearly 0.6 ± 0.2 mm/year and 0.3 ± 0.1 mm/year, respectively when $^{40}Ar/^{39}Ar$ K-feldspar ages (49 to 36 Ma) at Chang La[18] and our ZFT and AFT ages (42.0 and 25.0 Ma) are considered from the same elevation. Using AGE2EDOT program, it is evident that the maximum and minimum exhumation rates are further reduced to 0.25 and 0.1 mm/year respectively, within APR zone (see Figure 5) during 25.4 ± 2.6 to 9.2 ± 0.9 Ma (Figure 6). This agrees with ~0.1 mm/year rate from age-elevation plots (Figure 2)[45]. Thus, LB exhumed very slowly between Late Oligocene and Late Miocene when it crossed the ~115 ± 15°C geotherm. Since 9.0 Ma to present, its exhumation is somewhat accelerated to ~0.4 ± 0.1 mm/year.

Figure 7 *a*, *b* summarize the cooling and exhumation history of LB on the basis of our new and published data on many co-existing mineral pairs from the same samples with distinct two phases of enhanced exhumation during Middle Eocene and Late Miocene–Holocene. The batholith cooled and exhumed slowly during 43–42 to 10 Ma over a distance of more than 250 km, as is evident from the FT zircon–apatite ages from Kargil,

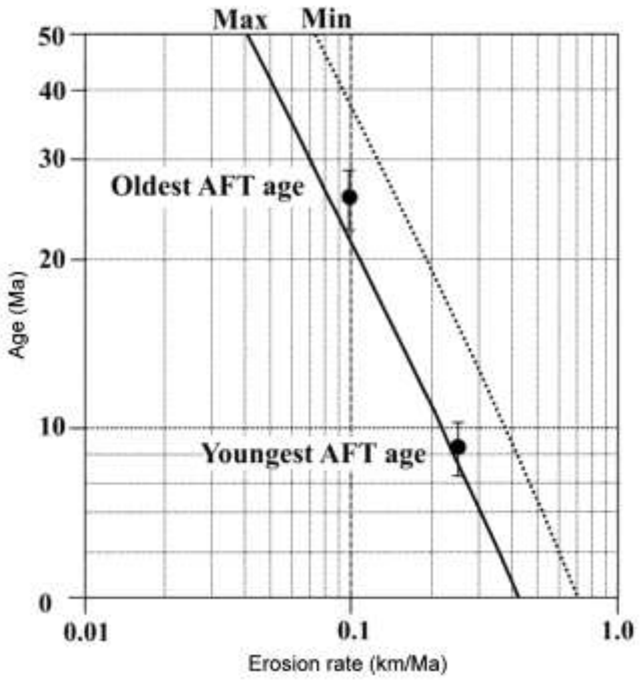

Figure 6. Growth curves of the AFT age and erosion rates of the Ladakh Batholith, using AGE2EDOT program. Maximum and minimum values are denoted by lower and upper curves.

Leh–Khardung La, Kharu–Chang La and Lyoma–Hanle sections. This scenario is similar to the Deosai Plateau, which was slowly cooling and exhuming since Eocene times[20].

Tectonic implications for the India–Asia convergence

Remarkable Early–Middle Eocene accelerated cooling and exhumation of LB near southern margin of the Asian Plate are closely linked to early convergence of the Kohistan–Ladakh arc with Indian continental lithosphere (ICL), when the latter also witnessed an early exhumation, possibly due to slab break-off of the Neo-Tethyan oceanic lithosphere[52]. After the event of slab-break off, slab-roll back mechanism came into play which must have been responsible for the fast rock uplift of LB as a whole. This has resulted in an overall fast and uniform exhumation of LB. This pulse is possibly linked to the exhumed leading edge of the Indian Plate in Tso Morari region. After the UHP metamorphism at *P*–*T* conditions of >3.9–3.5 GPa and >750°C at ~120 km depth and 53.3 ± 0.7 Ma (ref. 43) or ~55 ± 10 Ma (ref. 52) age, ICL buoyed up from deep mantle and underwent a record exhumation till ~48–45 Ma from ~120 km to 35 km (refs 43, 47, 52–55) through amphibolite facies. The lower greenschist facies minerals grew under 0.3 GPa and 200°C at 8 km between 45 ± 2 and 34 ± 2 Ma. Thus, the Tso Morari UHP terrain witnessed record maximum exhumation at 17 mm/year during ~53–50 Ma and subsequent deceleration to 12 mm/year (50–47 Ma), 0.3 mm/year till 34 ± 2 Ma (zircon FT age) and further down when it attained ~120°C around 24 ± 2 Ma (AFT ages)[43,56] (Figure 8). Close perusal of exhumation rates from LB, located on southern margin of the Asia Plate and adjoining eclogitized Indian continental lithosphere in Tso Morari reveals that both the terrains underwent fast exhumation during Eocene, though the latter exhumed much faster. This exhumation rate was transmitted to the batholith through various imbricated ophiolite-pelite-psammite-rich lithologies of the ITSZ (Figure 8).

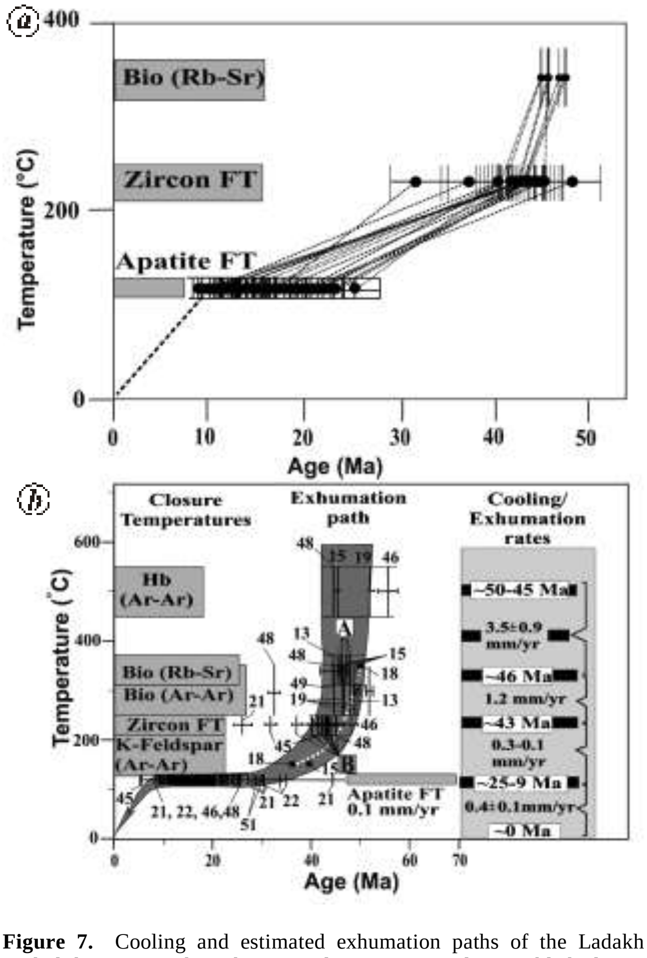

Figure 7. Cooling and estimated exhumation paths of the Ladakh Batholith. ***a***, New Rb–Sr biotite and FT zircon, and our published apatite FT data[45]. Tie lines for co-existing minerals in same samples. ***b***, Available published ages. Hornblende K–Ar/$^{40}Ar/^{39}Ar$[15,19,46,48]. Biotite Rb–Sr[13,Present data(A)]. Biotite K–Ar/$^{40}Ar/^{39}Ar$[13,15,19]. Zircon FT[21,45,Present data(B)]. K-feldspar $^{40}Ar/^{39}Ar$[15,18]. Apatite FT[19,21,22,46,48,51]. See text for details on closure temperatures.

Conclusions

After widespread magmatism at ~58 Ma and post-crystallization cooling, the Trans-Himalayan Ladakh Batholith witnessed fast Early–Middle Eocene cooling almost instantly from $^{40}Ar/^{39}Ar$ hornblende (500 ± 50°C) to Rb–Sr biotite (340 ± 30°C) closure temperatures between 52 ± 44 Ma and ~46.0 Ma respectively, at a very fast rate of ~105°C/Ma. It slowed down to 34 ± 13°C/Ma when it cooled to the ZFT closure temperature

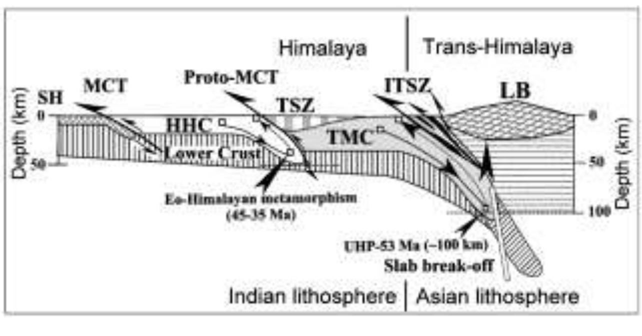

Figure 8. Schematic diagram of exhumation of the Ladakh Batholith and its relationship with the Indian continental lithosphere. Leading edge of the Indian continental lithosphere (lower crust-vertically-shaded and upper crust-grey shades) initially subducts steeply along the Indus-Tsangpo Suture Zone (ITSZ) and undergoes UHP metamorphism (downgoing arrows) at ~53 Ma. In the Higher Himalayan Crystallines (HHC), core of the Himalayan belt produced peak Eo-Himalayan metamorphism at ~45–35 Ma due to shallower continental lithospheric subduction along the proto-MCT. Eocene slab break-off of continental lithosphere causes exhumation of both the TMC and the HHC. The Sub-Himalaya (SH) is overridden by the HHC along the Main Central Thrust (MCT).

(230 ± 20°C) at ~43.0 Ma. It was possible due to an earlier tectonic exhumation at ~3.5 ± 0.9 mm/year till ~46 Ma (Rb–Sr biotite) and subsequent deceleration to ~1.2 ± 0.2 mm/year until 43–42 Ma (zircon FT ages) due to India–Asia convergence. This was also the period when leading northern eclogitized edge of the Indian continental lithosphere was undergoing exceedingly fast exhumation during HP and amphibolite facies metamorphism between 50 and 47 Ma respectively, as well as causing the Early–Middle Eocene exhumation of the overlying batholith. However, a Late Miocene–Holocene exhumation pulse is possibly caused by coupled tectonic-erosion processes within the Trans-Himalaya.

1. Platt, J. P., Exhumation of high-pressure metamorphic rocks: a review of concepts and processes. *Terra Nova*, 1993, **5**, 119–133.
2. Hodges, K. V., Parrish, R. R., Housh, T. B., Lux, D. R., Burchfiel, B. C., Royden, L. H. and Chen, Z., Simultaneous Miocene extension and shortening in the Himalayan orogen. *Science*, 1992, **258**, 1446–1470.
3. Ring, U., Horizontal contraction or horizontal extension: heterogeneous Late Eocene and Early Oligocene general shearing during blueschist and greenschist-facies metamorphism at the Pennine-Austroalpine boundary zone in the Western Alps. *Geol. Rundsch*., 1995, **84**, 843–859.
4. Ring, U., Brandon, M. T., Lister, G. S. and Willet, S., Exhumation processes. In *Exhumation Processes: Normal Faulting, Ductile Flow and Erosion* (eds Ring, U. *et al.*), Geol. Soc. London, Spec. Publ., 1999, vol. 154, 1–28.
5. Wobus, C. W., Hodges, K. V. and Whipple, K. X., Has focused denudation sustained active thrusting at the Himalayan topographic front? *Geology*, 2003, **31**, 861–864.
6. Searle, M. P. *et al.*, The closing of the Tethys and the tectonics of the Himalaya. *Geol. Soc. Am. Bull*., 1987, **98**, 678–701.
7. Jain, A. K., Kumar, D., Singh, S., Kumar, A. and Lal, N., Timing, quantification and tectonic modeling of Pliocene Quaternary movements in the NW Himalaya: evidences from fission track dating. *Earth Planet. Sci. Lett*., 2000, **179**, 437–451.
8. Montomoli, C., Carosi, R. and Salvatore, I., Tectonometamorphic discontinuities in the Greater Himalayan sequence: a local or a regional feature. In *Tectonics of the Himalaya* (eds Mukherjee, S. *et al.*), Geol. Soc. London Spec. Publ., 2014, **412**, 25–41.
9. Thiede, R. C. and Ehlers, T. A., Large spatial and temporal variations in Himalayan denudation. *Earth Planet. Sci. Lett*., 2013, **371–372**, 278–293.
10. Patel, R. C., Singh, S., Asokan, A., Manickavasagam, R. M. and Jain, A. K., Extensional tectonics in the collisional Zanskar Himalayan belt. In *Himalayan Tectonics* (eds Treloar, P. J., Searle, M. P.), Geol. Soc. London, Spec. Publ., 1993, **74**, 445–459.
11. Hodges, K. V., Bowring, S. A., Davidek, K. L., Hawkins, D. and Krol, M., Evidence for rapid displacement on Himalayan normal faults and the importance of tectonic denudation in the evolution of mountain ranges. *Geology*, 1998, **26**, 483–486.
12. Thiede, R. C., Arrowsmith, J. R., Bookhagen, B., McWilliams, M. O., Sobel, E. R. and Strecker, M. R., From tectonically to erosionally controlled development of the Himalayan orogen. *Geology*, 2005, **33**, 689–692.
13. Honegger, K., Dietrich, V., Frank, W., Gansser, A., Thoni, M. and Trommsdorff, V., Magmatism and metamorphism in the Ladakh Himalaya (the Indus-Tsangpo suture zone). *Earth Planet. Sci. Lett*., 1982, **60**, 253–292.
14. Hodges, K. V., Tectonics of the Himalaya and southern Tibet from two decades perspective. *Geol. Soc. Am. Bull*., 2000, **112**, 324–350.
15. Weinberg, R. F. and Dunlap, J., Growth and deformation of the Ladakh Batholith, Northwest Himalayas: Implications for timing of continental collision and origin of calcalkaline batholith. *J. Geol*., 2000, **108**, 303–320.
16. Rolland, Y., Pecher, A. and Picard, C., Middle Cretaceous back-arc formation and arc evolution along the Asian margin: the Shyok Suture Zone in Northern Ladakh (NW Himalaya). *Tectonophysics*, 2000, **325**, 145–173.
17. White, L. T., Ahmad, T., Ireland, T. R., Lister, G. and Forster, M. A., Deconvolving episodic age spectra from zircons of the Ladakh Batholith, northwest Indian Himalaya. *Chem. Geol*., 2011, **289**, 179–196.
18. Dunlap, W. J., Weinberg, R. F. and Searle, M. P., Karakoram fault zone rocks cool in two phases. *J. Geol. Soc. London*, 1998, **155**, 903–912.
19. Clift, P. D., Carter, A., Krol, M. and Kirby, E., Constraints on India-Eurasia collision in the Arabian sea region taken from the Indus Group, Ladakh Himalaya, India. In *The Tectonic and Climatic Evolution of the Arabian Sea Region* (eds Clift, P. D.), Geol. Soc. London, Spec. Publ., 2002, **195**, 97–116.
20. van der Beek, P., Van Melle, J., Guillot, S., Pêcher, A., Reiners, P. W., Nicolescu, S. and Latif, M., Eocene Tibetan plateau remnants preserved in the northwest Himalaya. *Nature Geosci*., 2009, **2**, 364–368.
21. Kirstein, L. A., Foeken, J. P. T., van der Beek, P., Stuart, F. M. and Phillips, R. J., Cenozoic unroofing history of the Ladakh Batholith, western Himalaya, constrained by thermochronology and numerical modelling. *J. Geol. Soc., London*, 2009, **166**, 1–12; doi:10.1144/0016-76492008-107.
22. Kirstein, L. A., Sinclair, H., Stuart, F. M. and Dobson, K., Rapid early Miocene exhumation of the Ladakh batholith, western Himalaya. *Geology*, 2006, **34**, 1049–1052.
23. Reiners, P. W., Todd A. E. and Zeitler, P. K., Past, Present, and future of thermochronology. *Rev. Mineral. Geochem*., 2005, **58**, 1–18.
24. Raz, U. and Honneger, K., Magmatic and tectonic evolution of the Ladakh block from field studies. *Tectonophysics*, 1989, **161**, 107–118.
25. Thakur, V. C., *Geology of the Western Himalaya*, Pergamon Press, Oxford, 1993, p. 355.
26. Scharer, U., Hamet, J. and Allegre, C. J., The Transhimalaya (Gangdese) plutonism in the Ladakh region: a U–Pb and Rb–Sr study. *Earth Planet. Sci. Lett*., 1984, **67**, 327–339.
27. Debon, F., Le Fort, P., Sheppard, S. M. F. and Sonet, J., The four plutonic belts of the Transhimalaya-Himalaya: a chemical, mineralogical, isotopic and chronological synthesis along a Tibet-Nepal section. *J. Petrol*., 1986, **27**, 219–250.
28. Kumar, S., Bora, S., Sharma, U. K., Yi, K. and Kim, N., Early Cretaceous subvolcanic calc-alkaline granitoid magmatism in the Nubra-Shyok valley of the Shyok Suture Zone, Ladakh Himalaya, India: evidence from geochemistry and U–Pb SHRIMP zircon geochronology. *Lithos*, http://dx.doi.org/10.1016/j.lithos.2016.11.019.
29. Gansser, A., The significance of the Himalayan suture zone. *Tectonophysics*, 1980, **62**, 37–52.
30. Le Fort, P., Himalayas: the collided range, present knowledge of the continental arc. *Am. J. Sci*., 1975, **275**, 1–44.
31. Rolland, Y., Picard, C., Pêcher, A., Lapierre, H., Bosch, D. and Keller, F., The cretaceous Ladakh arc of NW Himalaya – slab melting and melt – mantle interaction during fast northward drift of Indian Plate. *Chem. Geol*., 2002, **182**, 139–178.
32. Yin, A., Cenozoic tectonic evolution of the Himalayan orogen as constrained by along-strike variation of structural geometry, exhumation history, and foreland sedimentation. *Earth Sci. Rev*., 2006, **76**, 1–131.
33. Jain, A. K., Singh, S. and Gupta, K. R., A Late Cretaceous Karakoram Shear Zone and its reactivation during the Late Cenozoic. *Int. Assoc. Gondwana Res. Mem*., 2007, **10**, 77–88.

34. Jain, A. K. and Singh, S., *Geology and Tectonics of the Southeastern Ladakh and Karakoram.* Geological Society of India, Bangalore, 2009, pp. 179.
35. Jain, A. K., Continental subduction in the NW-Himalaya and Trans-Himalaya. *Ital. J. Geosci*., 2016, **135**(2), doi: 10.3301/IJG.2015.43.
36. Singh, S., Kumar R., Barley, M. and Jain, A. K., U–Pb SHRIMP ages and depth of emplacement of Ladakh Batholith, NW Himalaya. *J. Asian Earth Sci*., 2007, **30**, 490–503.
37. St-Onge, M. R., Rayner, N. and Searle, M. P., Zircon age determinations for the Ladakh batholith at Chumathang Northwest India: implications for the age of the India–Asia collision in the Ladakh Himalaya. *Tectonophysics*, 2010, **495**, 171–183.
38. Jain, A. K., When did India–Asia collide and make the Himalaya? *Curr. Sci.*, 2014, **106**(2), 254–266.
39. Jain, A. K., Singh, S., Manickavasagam, R. M., Joshi, M. and Verma, P. K., HIMPROBE Programme: Integrated studies on geology, petrology, geochronology and geophysics of the Trans-Himalaya and Karakoram. *Mem. Geol. Soc. India*, 2003, **53**, 1–56.
40. Jain, A. K. and Singh, S., Tectonics of the southern Asian Plate margin along the Karakoram Shear Zone: Constraints from field observations and U–Pb SHRIMP ages. *Tectonophysics*, 2008, **451**(1–4), 186–205.
41. Maheo, G., Bertrand, H., Guillot, S., Villa, I. M., Keller, F. and Capiez, P., The south Ladakh ophiolites (NW Himalaya, India): an intra-oceanic tholeiitic origin with implication for the closure of the Neo-Tethys. *Chem. Geol*., 2004, **203**, 273–303.
42. Ahmad, T., Tanaka, T., Sachan, H. K., Asahara, Y., Islam, R. and Khanna, P. P., Geochemical and isotopic constraints on the age and origin of the Nidar Ophiolitic Complex, Ladakh, India: Implications for the Neo-Tethyan subduction along the Indus suture zone. *Tectonophysics*, 2008, **451**, 206–224.
43. Leech, M. L., Singh, S. and Jain, A. K., Continuous metamorphic zircon growth and interpretation of U–Pb SHRIMP Dating: an example from the Western Himalaya. *Int. Geol. Rev*., 2007, **49**, 313–328.
44. Guillot, S., Replumaz, A., Hattori, K. and Strzerzynski, P., Initial geometry of western Himalaya and ultrahigh pressure metamorphic evolution. *J. Asian Earth Sci.*, 2007, **30**, 557–564.
45. Kumar, R., Lal Nand, Singh Sandeep and Jain, A. K., Exhumation history of Trans-Himalayan Ladakh Batholith as constrained by fission track apatite and zircon ages. *Curr. Sci*., 2007, **92**(4), 490–496.
46. Sorkhabi, R. B., Jain, A. K., Nishimura, S., Itaya, T., Lal, N., Manickavasagam, R. M. and Tagami, T., New age constraints on the cooling and unroofing history of the Trans Himalayan Ladakh batholith (Kargil area), N. W. India. *Proc. Indian Acad. Sci.* (*Earth Planet. Sci.*), 1994, **103**, 83–97.
47. Bouilhol, P., Jagoutz, O., Hanchar, J. M. and Dudas, F. O., Dating the India–Eurasia collision through arc magmatic records. *Earth Planet. Sci. Lett*., 2013, **366**, 163–175.
48. Schlup, M., Carter, A., Cosca, M. and Steck, A., Exhumation history of eastern Ladakh revealed by ^{40}Ar/^{39}Ar and fission track ages: the Indus river-Tso Morari transect, NW Himalaya. *J. Geol. Soc. London*, 2003, **160**, 385–399.
49. Bhutani, R., Pande, K. and Venkatesan, T. R., Tectono-thermal evolution of the India–Asia collision zone based on ^{40}Ar–^{39}Ar thermochronology in Ladakh. India. *Proc. Indian Acad. Sci*., 2004, **113**, 737–754.
50. Clift, P. D., Shimizu, N., Laynge, G., Gaedicke, C., Schulter, H. U., Clark, M. and Amjad, S., Development of the Indus Fan and its significance for the erosional history of the western Himalaya and Karakoram. *Geol. Soc. Am. Bull.*, 2001, **113**, 1039–1051.
51. Sinclair, H. D. and Jaffey, N., Sedimentology of the Indus Group, Ladakh, Northern India: implications for the timing of initiation of paleo-Indus River. *J. Geol. Soc. London*, 2001, **158**(1), 151–162.
52. Kohn, M. J. and Parkinson, C. D., Petrological case for Eocene slab breakoff during the Indo-Asian collision. *Geology*, 2002, **30**(7), 591–594.
53. de Sigoyer, J. *et al.*, Dating the Indian continental subduction and collisional thickening in the northwest Himalaya: multichronology of the Tso Morarieclogites. *Geology*, 2000, **28**, 487–490.
54. Leech, M. L., Singh, S., Jain, A. K., Klemperer, S. L. and Manickavasagam R. M., Early, steep subduction of India beneath Asia required by early UHP metamorphism. *Earth Planet. Sci. Lett*., 2005, **234**, 83–97.
55. Guillot, S., Mahéo, G., de Sigoyer, J., Hattori, K. H. and Pêcher, A., Tethyan and Indian subduction viewed from the Himalayan high-to ultrahigh-pressure metamorphic rocks. *Tectonophysics*, 2008, **451**, 225–241.

ACKNOWLEDGEMENTS. Thanks are due to DST, New Delhi for funding two research projects on National Facility on Isotope Geology/Geochronology and HIMPROBE for which we are grateful to the late K.R. Gupta and dedicate this work in his memory. A.K.J. thanks the JSPS Fellowship and K. Arita (Hokkaido University, Japan) and the INSA Senior Scientist Scheme at the CSIR-Central Building Research Institute, Roorkee where this work was completed. This manuscript is greatly benefited by comments from O. N. Bhargava, Mary Leech, R. Weinberg, J. P. Platt, Stephen Guillot, K. Arita and two anonymous reviewers. Thanks are due to N. V. Chalapathi Rao for editorial handling of the manuscript. R.K. acknowledges the Head, Department of Earth Sciences, IIT Roorkee, Roorkee for extending the facilities and CSIR, New Delhi for a Senior Research Fellowship at IIT Roorkee.

Received 10 November 2016; revised accepted 18 April 2017

doi: 10.18520/cs/v113/i06/1090-1098